WORLD CONFERENCE ON TIMBER ENGINEERING 2025
BRISBANE, AUSTRALIA
Advancing Timber for the Future Built Environment

Vibration Tests on Long-Span CLT-GLT Composite Floors

Amin Nabati [1], Sovanroth Ou[2], Muzan Williams Ijeoma[3], Weichiang Pang[4], Michael Stoner[5], Brandon Ross[6], Dustin Albright[7], Patricia Layton[8], Mik Carbajales-Dale[9]

ABSTRACT: In this study, the vibrational behaviour of two full-scale composite floor systems, each 12.2 m (40 ft) long, made of Cross-Laminated Timber (CLT) and Glued-Laminated Timber (GLT) with office use under heel drop excitation has been investigated. The primary aims include studying composite structures' natural frequencies, mode shapes, and damping. Additionally, the effects of openings in GLT and CLT on vibrational behaviour will be discussed. Experimental vibration tests are conducted for two composite floor systems with different types of connections, including screws with glue and screw with sharp metal before and after making the opening. The results show that openings in CLT and GLT have negligible effects on the vibration behaviour of the composite system.

KEYWORDS: Timber, Vibration, CLT, GLT, Composite floor, heel-drop

1 – INTRODUCTION

Recent progress in fabricating engineered wood products (EWPs), such as CLT and GLT, has encouraged researchers and engineers to consider mass timber as a competitive construction material for multi-story buildings. Sustainability, carbon sequestration, lightweight nature, high strength-to-weight ratio [1], and fast, dry construction [2] are reasons for using these elements in modern constructions. Lately, there has been a growing tendency toward using mass timber in low-rise and mid-rise buildings in the United States following the adoption of the most recent updates of the International Building Code (IBC) [3].

Compared with common materials such as concrete and steel, EWPs are well-known for their lighter weight and lower damping ratio, categorising them as vibration-sensitive due to human excitations [4]. Additionally, the demand for long-span floors is increasing due to the need for open spaces, especially in office building occupancies where open spaces are essential, but there are still some limitations to designing and constructing these types of floors. On the other hand, the design of spans over 6 m is controlled by serviceability rather than strength, highlighting the importance of a precise assessment of long-span floor systems [5].

Considering the composition of CLT and GLT as a solution for higher spans, a composite floor system comprised of a CLT panel with 2.44 m (8 ft) at the top as the top flange, two GLT beams at the middle as the webs, and one 1.83 m (6 ft) CLT panel at the bottom as the bottom flange with a 12.2 m (40 ft) length of clear span with new types of connections such as screws with adhesive and screws with sharp metal has been proposed (*FIG. 1*). The space inside

1 Amin Nabati, Glenn Dept. of Civil Engineering, Clemson University, Clemson, USA, anabati@clemson.edu

2 Sovanroth Ou, Glenn Dept. of Civil Engineering, Clemson University, Clemson, USA, sovanro@clemson.edu

3 Muzan Williams Ijeoma. Dept. of Environmental Engineering and Earth Sciences, Clemson University, Clemson, USA, mijeoma@clemson.edu

4 Weichiang Pang, Glenn Dept. of Civil Engineering, Clemson University, Clemson, USA, wpang@clemson.edu

5 Michael Stoner, Glenn Dept. of Civil Engineering, Clemson University, Clemson, USA, mwstone@clemson.edu

6 Brandon Ross, Glenn Dept. of Civil Engineering, Clemson University, Clemson, USA, bross2@clemson.edu

7 Dustin Albright, School of Architecture, Clemson University, Clemson, USA, dalbrig@clemson.edu

8 Patricia Layton, Forestry and Environmental Conservation Dept., Clemson University, Clemson, USA, playton@clemson.edu

9 Mik Carbajales-Dale, Dept. of Environmental Engineering and Earth Sciences, Clemson University, Clemson, USA, madale@clemson.edu,

https://doi.org/10.52202/080513-0054

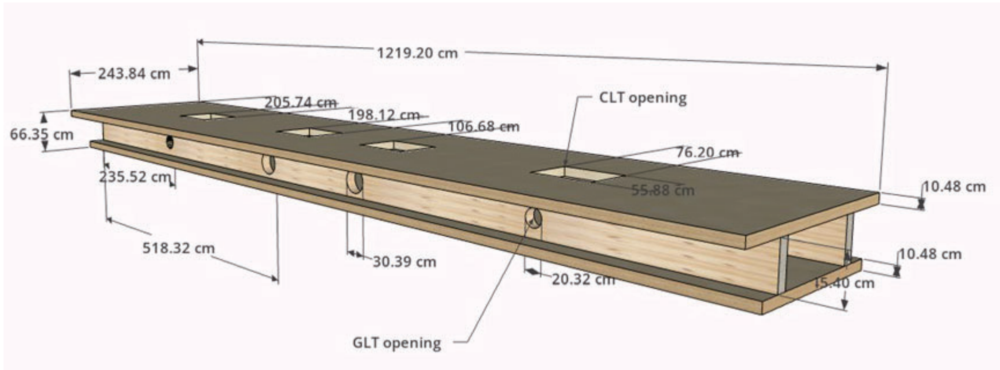

Figure 1: Timber floor system overall view and dimensions

the floor system and between CLTs and GLTs has been designed to accommodate MEP (Mechanical, Electrical, Piping) systems and the shorter width of the bottom panel allows for better access to these systems. While the combination of CLT and GLT offers higher structural performance, the vibrational characteristics of these composite floor systems have not been fully understood completely, especially when using novel types of connections. Additionally, the effects of openings in vibrational behaviours have not been studied. These understandings of vibrational behaviour will ensure that office building residents are comfortable with this composite floor system. This paper explores the modal properties of two composite floor systems, including the natural frequencies, damping ratios, and mode shapes due to the heel drop test. Furthermore, a previously proposed method for estimating the frequency has been compared with experimental results.

2 – BACKGROUND

With the advent of new materials and composite structures in recent years and the need for more extended floor spans, greater attention has been paid to floor vibration behaviour and its impact on building performance, particularly on timber floors, where human comfort is more affected due to their susceptibility to vibrations. Studies have shown that the material properties of CLT and GLT, span length, and inter-panel connections influence vibration performance.

2.1 Vibration of timber floors

Some studies focused on the vibration behavior of EWPs, while others focused on their combination. Gu et al. studied the vibration behaviour of CLT panels with different supports. They concluded that the stiffness of the support has an enormous influence on the vibration behaviour of CLT panels in such a way that decreasing the stiffness of the support reduces the fundamental natural frequency of CLT [6]. A study by Slotboom et al. [7] explored the modal properties of a long-span office CLT-GLT timber floor system. They reported that the timber floor behaved as a high-frequency floor (8.5 Hz), and adding a concrete topping increased the mass, considerably decreasing the frequency to 6 Hz. By adding some partitions and furnishing, they reported a slight increase in frequency, which was primarily related to an increase in stiffness. They also concluded a noticeable variation (30-40%) in frequency prediction between pinned and fixed supports due to floor system stiffness change. In another study, researchers investigate the vibration of a long-span lightweight 6m×6m timber floor. They reported the frequency of the floor as 9.08 Hz, which agreed with the numerical results. They also reported significant inconsistencies across codes regarding floor acceptance levels [5]. Hamm et al. [8] experimentally tested and numerically modelled various long-span (8 m-12 m) timber floors with different support conditions. They concluded that traditional vibration design codes are insufficient for evaluating the vibrations of long-span floor systems and the natural frequency is affected by floor mass, floor stiffness, span length, and whether the support is elastic or stiff.

Connections in EWPs play a crucial role in vibration performance on timber floors and are integral to energy dissipation mechanisms. In one study, Mazelli et al. [9] investigated the effects of the stiffness of inclined screws on the vibration behaviour of timber-to-timber connections. They concluded that increasing connection stiffness, achieved by increasing the inclination angle from 0° (vertical screws) to 45° (inclined screws), leads to an increase in the fundamental frequency of the floor. In another study, Zhang et al. [10] explored how the CLT-steel beam connection affects the vibration behaviour of the composite system. They found that the natural

https://doi.org/10.52202/080513-0054

frequency and damping ratio are not significantly affected by the diameter or length of the screws. However, the distances among screws were found to be effective on the fundamental frequency.

There are a few studies regarding the effects of openings on structural performance in timber structures. Karimi et al. [11] tested timber-timber composite (TTC) beams with CLT as the top flange and GLT as the web. They explored the effects of different parameters such as opening shapes (square and circular openings), screw sizes, and the continuity of the CLT. They found that an opening with 62.5% of the web depth had little effect on the stiffness of the beam, with a reduction of 4% in stiffness for specimens with the opening. A significant reduction (23-30%) was reported for specimens with discontinuous CLTs.

2.2 DG11 guidelines for evaluating the frequency

In AISC Design Guide 11 [12], a method is proposed for estimating the natural frequency of simply supported beams and girders with uniform mass based on midspan deflection:

$$f_n = 0.18\sqrt{\frac{g}{\Delta}} \tag{1}$$

where g is the acceleration due to gravity (9.81 m/s^2), and $\mathbf{\Delta}$ (m) is the midspan deflection of the member due to self-weight. This deflection can be modified to represent the composite system's deflection by replacing the bending stiffness in the original formula with that of the composite section, which is equal to:

$$\Delta = \frac{5wl^4}{384EI_{comp.}} \tag{2}$$

where w is the actual self-weight of the floor per unit length (kN/m), l is the span length (m), and $EI_{comp.}$ is the bending stiffness of the timber composite section. This composite stiffness is calculated based on the apparent bending stiffness of the CLT ($EI_{app.}$) introduced in the CLT Handbook [13] and the bending stiffness of the GLT ($EI_{GLT.}$).

3 – PROJECT DESCRIPTION

3.1 Design, Materials and Construction

To develop a reliable structural performance that complies with design standards, the mechanically jointed beam theory presented in Eurocode 5 has been selected to design the composite floor system. Additionally, for calculating the stiffness and shear capacity of GLTs with openings, APA V700E guidelines have been used.

The experimental setup involves the fabrication of two full-scale CLT-GLT composite floor systems, one with screws and adhesive and the other with screws and sharp metal. Each floor system consists of two V3-3alt CLT panels at the top and bottom of the specimens and two 24F-V5M1 GLTs as the web of the composite section manufactured by SMARTLAM.

For fabricating the adhesive-with-screw specimen, CLT panels were connected to GLTs using SIMPSON SDCF27912 screws and Loctite PL Premium Max Adhesive between them. On the other hand, for the sharp-metal-with-screw specimens, ROTHOBLASS TBS822 screws with LS13373 washers and ROTHOBLASS SHARP501200 sharp metal were used. The washers were used to exert enough clamping pressure for the sharp metal to penetrate CLT and GLT. To build each specimen, two 12.8 m (42 ft) long glulam beams were placed on the 12.8 m (42 ft) by 1.83 m (6 ft) CLT panel (bottom panel) after applying some adhesive or placing sharp metal and then screws were driven in from the bottom of the lower CLT panel (FIG. 2). Then, the adhesive or sharp metal was placed on the top of the GLTs, and the 12.8 m (42 ft) by 2.44 m (8 ft) CLT panel (top CLTs) was placed on the top of the assembly. In the next step, screws were driven into the CLTs and GLTs from the top side of the CLT. In the last step, four openings in each GLT and four openings in the top CLT panel were drilled (Fig. 3).

Figure 2: Specimen after placing GLTs on the top of the bottom CLT

Figure 3. Specimen after construction

https://doi.org/10.52202/080513-0054

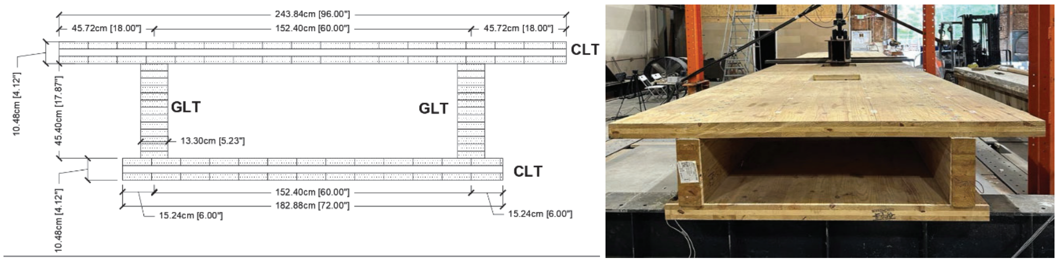

Figure 4: The dimensions of the cross-section for both assembly specimens and the specimen after construction

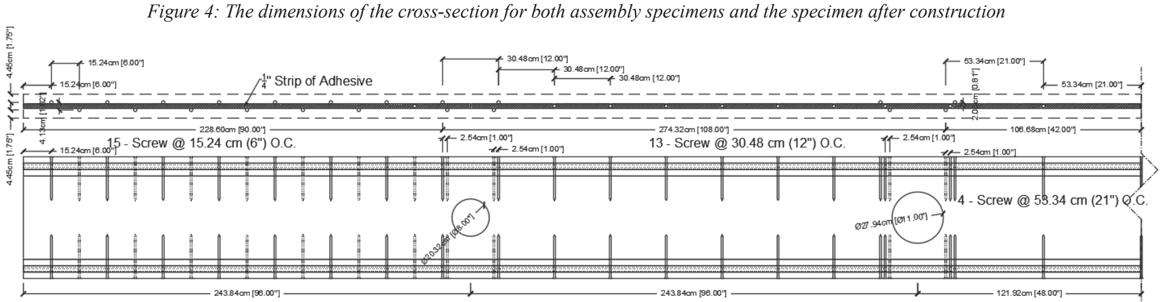

Figure 5 : Adhesive plus screw connection details

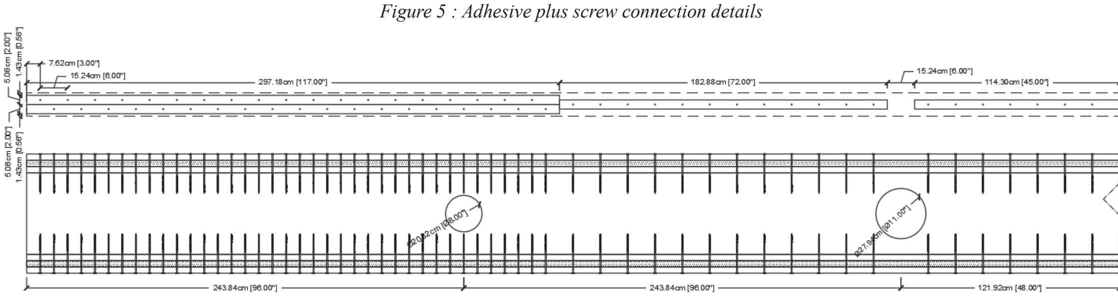

Figure 6 : Sharp metal plus screw connection details

The dimensions of the cross-section and cross-section after construction are shown in *Fig.* ***4***. Additionally, the details of the connections are depicted in *Fig.* **5** and *Fig.* ***6***.

3.2 Vibration Measurements

After completing the fabrication, a modal test was carried out to obtain the vibration characteristics of the composite floor system. The vibration test setup included a force plate with two steel plates, one at the top and one at the bottom, and three OMEGA (LC401-1K) load cells between these steel plates, each with a capacity of ±1000 lbf. These load cells were connected to a NI9234 module, and the data were recorded through the NI cDAQ and NIMAX (National Instrument Measurement & Automation Explorer) software interface. Additionally, 12 PCB Piezotronics accelerometers (model 333B50) were selected to collect the floor acceleration data. These accelerometers were connected to three NI9237 modules, and the data were recorded. A schematic view of the vibration setup is presented in *Fig. 7*. To record the acceleration data of the floor, 84 representative points were selected on the top CLT panel and marked at intervals of 0.61 m (2 ft) from each other (*Fig. 8*). For each modal test, which was conducted using a group of 12 sensors, first, a person stands on the force plate, balances on their toes, and then brings his heels down, which causes enough excitation for the floor to vibrate (*Fig.* ***9***). Then, this procedure is repeated seven times to cover the 84 points on the floor entirely. For each test, acceleration-time data from accelerometers and force data from steel plates were collected during heel-drop tests.

Vibration tests were performed in several steps to explore the effects of the openings on the composite floor system. Initially, the vibration tests were conducted on specimens without any openings, then two openings near the centre of the specimen were cut into the GLTs, and then vibration tests were performed. In the next step, the other two additional openings were cut, and while the specimen now having four openings in each GLT, the vibration tests were conducted again. In the final step, all openings in CLT were made, and the vibration test was repeated. This process is shown in *Fig.* ***10***.

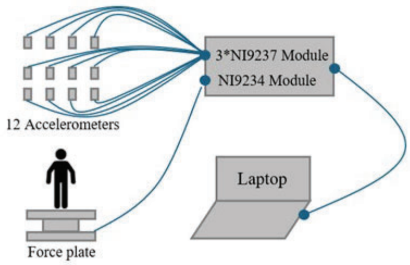

Figure 7: Schematic view of vibration test setup

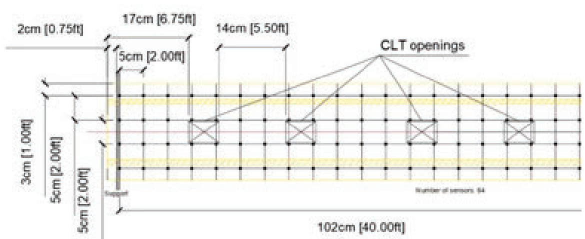

Figure 8: Accelerometer location plan

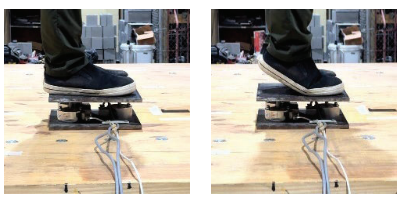

Figure 9: Heel drop test

3.2 Theoretical Background

After collecting the data, the modal frequencies, damping ratios, and mode shapes were explored and extracted from the Frequency Response Function (FRF) [14]. The FRF describes how the structure responds to a dynamic excitation and is typically calculated using input and output signals by dividing the response (acceleration) at location j by excitation (heel-drop) at location i as:

$$H_{ij}(j\omega) = \frac{A_j(j\omega)}{F_i(j\omega)} \tag{3}$$

in which $A_j(j\omega)$ is the Fourier transform of the measured acceleration at point j, $F_i(j\omega)$ is the Fourier transform of the applied force at point i, and $H_{ij}(j\omega)$ is the FRF in the frequency domain between points i and j [15]. The frequencies of the peaks in the FRF plot can be identified as natural frequencies, which indicate the system's resonance frequencies [16].

Theoretically, the FRF can be stated in modal form as:

$$H_{ij}(j\omega) = \sum_{k=1}^{N} \frac{u_i^{(k)} u_j^{(k)}}{-\omega^2 + 2j\xi_k\omega_k\omega + \omega_k^2} \tag{4}$$

where N is the total number of modes, $u_i^{(k)}$ is the mode shape component at the excitation point for the K-th mode, $u_j^{(k)}$ is the mode shape components at the response points for the c, ω_k is the natural circular frequency (rad/s) of the k-th mode, ω is the excitation frequency and ξ_k is the damping ratio of the k-th mode [14], [17]. At each resonance frequency, the response is dominated by a single mode, and the FRF formula simplifies to:

$$H_{ij}(j\omega) \approx \frac{a_k}{j\omega - (j\omega_k - \sigma_k)} + \frac{a_k^*}{j\omega - (j\omega_k + \sigma_k)} \tag{5}$$

in which a_k is the residue that embeds mode shape data, $\sigma_k = \xi_k\omega_k$ is the modal damping term, and a_k^* is the complex conjugate of a_k. The mode shape data can be extracted by analyzing the imaginary part of the FRF. At resonance, the imaginary part of the FRF reaches its maximum, and the peak value directly relates to the residue according to the following equation:

$$a_k = q_k u_i^{(k)} u_j^{(k)}$$

in which q_k is a scaling factor. The peak values of the imaginary part of the FRFs for all measured points can be used to extract the mode shape of the structure. After normalizing the values, these peak values form the approximate shape of the mode based on the peak-picking technique [16]. Using this method and MATLAB code, the mode shapes of both floor systems were extracted.

After finding natural frequencies and mode shapes, the FRFs were used to estimate the damping ratio of the floor system using the half-power bandwidth method at resonance peaks. The classical formula for calculating damping is:

$$\xi = \frac{\omega_b - \omega_a}{2\omega_n} \tag{6}$$

4 – RESULTS

4.1 Natural frequencies of composite floor

Table 2 summarizes the natural frequencies of two types of composite timber floor systems: adhesive with screws and sharp metal with screws. Each type includes four specimens: 'WO' (without openings), 'G2' (GLT with two openings in the middle), 'G4' (GLT with four openings), and 'G4C4' (GLT with four openings and CLT with four openings). As mentioned in the previous section, all acceleration-time data were transferred from the time domain into the frequency domain. The peak points represent the first three frequencies of the structure in *Fig. 11* which is for the adhesive and screw.

https://doi.org/10.52202/080513-0054

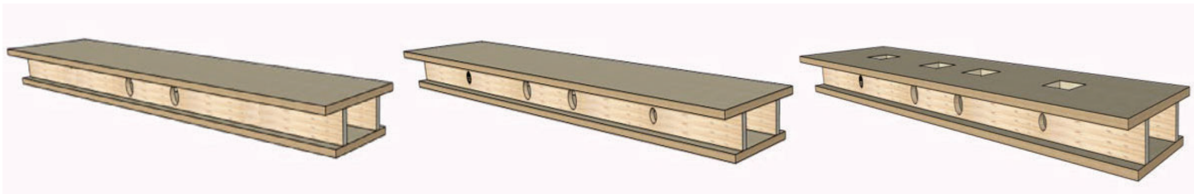

Figure 10: Floor systems with two openings in GLT, four openings in GLT, four openings in GLT and four openings in CLT (from left to right)

Table 2 shows that slight frequency differences between specimens with and without openings were attributed to uncertainties in each vibration test. These results imply that the variations in weight and stiffness are such that the frequencies remain almost constant, and nearly the same weight and stiffness of the specimen are activated during the vibration. Regarding weight, cutting four openings in CLT has the most impact on the weight of the composite floor, reducing it by 3.2% of the total weight. Also, for each GLT, openings had less effect on the structure's weight, each with 0.4% of the total weight. Considering all openings, they decrease the weight of the structures by 4%.

As stated in section 2.2, to calculate the frequency of the floor system, first $EI_{comp.}$ was calculated, then using equation (2), the deflection of the composite beam was calculated, and finally, using equation (1), the frequency was extracted. To calculate the $EI_{app.}$ of CLTs, the factory datasheet values for $EI_{eff.}$ and $GA_{eff.}$ according to Table 1 were used.

Table 1 : CLT material properties

Property	Value (Imperial)	Value (SI)
$EI_{eff.}$	$95 \times 10^6 \dfrac{\text{lbf} * \text{in}^2}{\text{ft}}$	$895{,}283 \dfrac{\text{N} * \text{m}^2}{\text{m}}$
$GA_{eff.}$	$49 \times 10^4 \dfrac{\text{lbf}}{\text{ft}}$	$7.15 \times 10^6 \dfrac{\text{N}}{\text{m}}$

The calculated value for natural frequency was 9.09 Hz, based on full composite assumption and almost the same as the experimental values. The difference between the calculated frequency and the experimental one was around 3.5%. This aligns with our knowledge that the adhesive with screws behaves more like a full composite section than the sharp metal specimen.

4.2 Damping ratio of composite floor

There are two primary sources for damping in timber floors, according to Hu et al. [19]: Material Damping, related to the inherent damping of wood and Fractional Damping, due to connections, friction between different components and boundary connections at supports. The latest is the dominant of the two primary sources, which means most of the damping of the composite floor system comes from connections. The combination of sharp metal and screws provide frictional energy dissipation between timber and sharp metal while adding adhesive prevents slip which limits the mechanism for contributing to damping. This means we should expect higher damping for sharp metal specimens in comparison with the specimen with adhesive and screws. The half-power bandwidth method was used to calculate the damping ratio of specimens, and the results show that the damping ratio for the first mode for adhesive with screw specimens is 1.42%. In contrast, for sharp metal with screw specimens, it is 2.1%. Since we have four rows of connections, the damping ratio is higher than the standard damping ratio for timber floors, which is around 1% [19]. Additionally, higher modes have a smaller damping ratio, which can be due to smaller and more localized deformations of the connections, consequently reducing the participation of connections in damping [18]. In Table 3, all of the damping ratios are shown.

4.3 Mode shape of composite floor

As discussed in the previous section, mode shapes were extracted using the aforementioned theoretical method. The first three mode shapes for each specimen are shown in FIG. 12 to FIG. 17. Three different mode shapes characterized the dynamic behaviour of the composite timber floor. In the first mode shape, the entire floor system experienced global bending about the short axis at the middle of the floor plan. So, the first mode of the system is the first bending moment. This mode shape is the most significant mode shape from a serviceability point of view because the overall dynamic response of the floor is highly tied to this mode shape. In the second mode shape, the entire floor exhibited an out-of-plan rotation about the longitudinal axis at the middle of the floor. So, the second mode shape of the system is the first torsional mode shape. Like mode one, the third mode represented the bending mode with an additional nodal line along its width. So, the third mode is the second bending mode shape. These mode shapes have been reported before by Ussher et al. [20] for CLT floors.

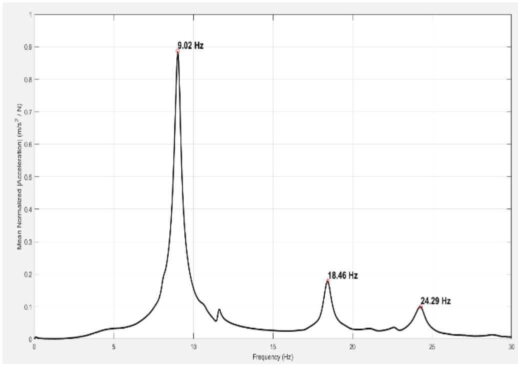

Figure 11 : Floor acceleration-frequency response for all the accelerometers: Adhesive-screw

Table 2 : frequencies of floor system with different openings for adhesive-screw and sharp metal-screw specimens.

Specimen		1st Mode frequency	2nd Mode frequency	3rd Mode frequency
Adhesive +screw	WO	9.02	18.46	24.29
	G2	9.2	18.67	24.36
	G4	9.14	18.67	24.36
	G4C4	9.02	18.59	24.28
Sharp metal +screw	WO	8.78	17.76	24.1
	G2	8.84	17.8	23.81
	G4	8.84	17.74	24.65
	G4C4	8.78	17.37	24.35

Table 3 : Damping ratios of floor system with different openings for adhesive-screw and sharp metal-screw specimens

Specimen		Mode 1	Mode 2	Mode 3
Adhesive+screw	WO	1.42	1.1	1.1
	G2	1	1.27	1.15
	G4	1.21	1.18	1.2
	G4C4	1.41	1.28	1.12
Shap metal+screw	WO	2.1	1.44	1.4
	G6	1.2	1.2	1.14
	G8	1.45	1.24	1.18
	G4C5	1.47	1.16	0.9

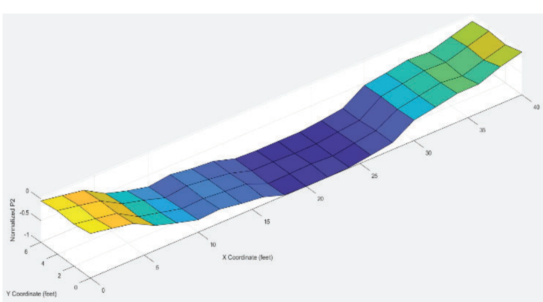

Figure 12: First bending mode of the adhesive-screw floor (Mode 1)

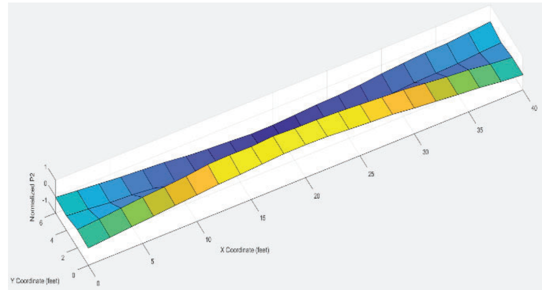

Figure 13: First torsional mode of the adhesive-screw floor (Mode 2)

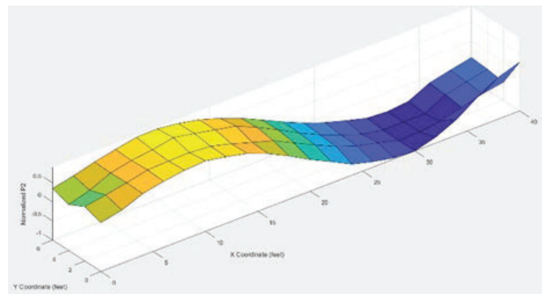

Figure 14: Second bending mode of the adhesive-screw floor (Mode 3)

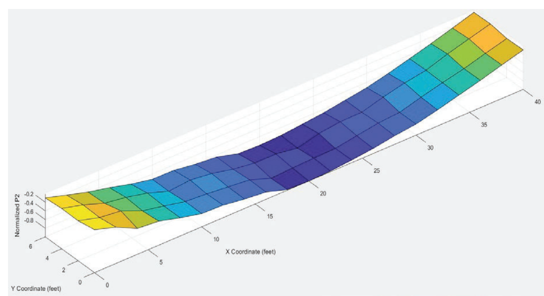

Figure 15: First bending mode of the sharp metal-screw floor (Mode 1)

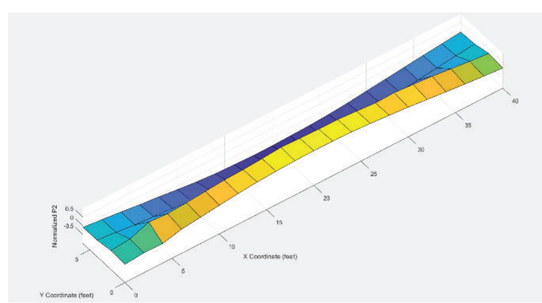

Figure 16: First torsional mode of the metal-screw floor (Mode 2)

https://doi.org/10.52202/080513-0054

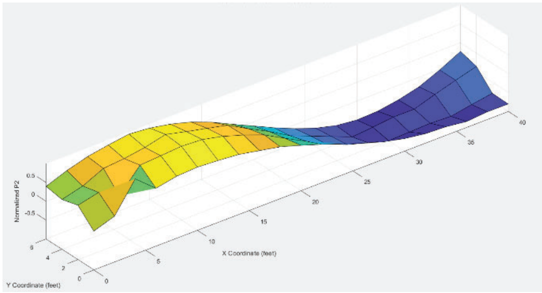

Figure 17: Second bending mode of the sharp metal-screw floor (Mode 3)

5 – CONCLUSION

This research explores the vibrational behavior of two long-span composite CLT-GLT timber floor systems with two different types of connections, including adhesive with screws and sharp metal with screws. The study revealed that openings have minimal effect on the vibrational behaviour of the specimens, and despite introducing multiple openings, the overall dynamic characteristics haven't changed significantly. Also, the damping ratio of the timber floor for both connections was higher than that of the typical timber floors, which implies the efficiency of this specimen in dissipating energy. Also, the damping ratio for the sharp metal specimen was higher than the adhesive one. Additionally, the comparison between the two types of connections shows that the adhesive-screw specimen has a higher frequency. Also, the mode shapes of the two specimens without openings are similar. Also, DG11 prediction for frequency has an acceptable value.

6 – REFERENCES

[1] M. H. Ramage *et al.*, "The wood from the trees: The use of timber in construction," *Renewable and Sustainable Energy Reviews*, vol. 68, pp. 333–359, Feb. 2017, doi: 10.1016/j.rser.2016.09.107.

[2] J. Zhou and Z. Zhao, "Apparent impact sound insulation performance of cross laminated timber floors with floating concrete toppings," *INTER-NOISE and NOISE-CON Congress and Conference Proceedings*, vol. 263, no. 1, pp. 5203–5215, Aug. 2021, doi: 10.3397/IN-2021-3006.

[3] P. Nepal, J. P. Prestemon, I. Ganguly, V. Kumar, R. D. Bergman, and N. C. Poudyal, "The potential use of mass timber in mid-to high-rise construction and the associated carbon benefits in the United States," *PLoS One*, vol. 19, no. 3, p. e0298379, Mar. 2024, doi: 10.1371/journal.pone.0298379.

[4] A. Opazo-Vega, F. Muñoz-Valdebenito, and C. Oyarzo-Vera, "Damping Assessment of Lightweight Timber Floors Under Human Walking Excitations," *Applied Sciences*, vol. 9, no. 18, p. 3759, Sep. 2019, doi: 10.3390/app9183759.

[5] H. Karampour *et al.*, "DESIGN OF LONG-SPAN LIGHTWEIGHT TIMBER FLOORS SUBJECT TO WALKING EXCITATIONS: A CASE STUDY," in *World Conference on Timber Engineering (WCTE 2023)*, As, Norway: World Conference on Timber Engineering (WCTE 2023), 2023, pp. 1873–1879. doi: 10.52202/069179-0247.

[6] C. Guo and J. Zhou, "VIBRATION SERVICEABILITY PERFORMANCE OF MASS TIMBER FLOORS UNDER VARIOUS SUPPORT CONDITIONS," in *13th World Conference on Timber Engineering, WCTE 2023*, World Conference on Timber Engineering (WCTE), 2023, pp. 1921–1929. doi: 10.52202/069179-0254.

[7] C. Slotboom, C. Dickof, and T. Fast, "EXPERIMENTAL AND NUMERICAL ASSESSMENTS OF A LONG-SPAN MASS TIMBER FLOOR SYSTEMS SUBJECTED TO FOOT-FALL INDUCED VIBRATION."

[8] P. Hamm, V. Knöpfle, J. Ruf, P. Bacher, and T. Götz, "FULL SCALE VIBRATION TESTS ON A LONG SPAN TIMBER FLOOR."

[9] A. Mazelli and C. Bedon, "Sensitivity of human-induced vibrations and comfort analysis to partially rigid STS joints in timber-to-timber composite floors," *Measurement (Lond)*, vol. 228, Mar. 2024, doi: 10.1016/j.measurement.2024.114396.

[10] J. Zhang, C. Zhang, Y. Li, W. S. Chang, and H. Huang, "Cross-laminated timber (CLT) floor serviceability under multi-person loading: Impact of beam–panel connections," *Eng Struct*, vol. 296, Dec. 2023, doi: 10.1016/j.engstruct.2023.116941.

[11] A. Karimi-Nobandegani and H. Valipour, "Effect of web openings on timber composite beams: Testing and analytical modelling," *Eng*

Struct, vol. 256, Apr. 2022, doi: 10.1016/j.engstruct.2022.114064.

[12] T. M. Murray, D. E. Allen, E. E. Ungar, and D. Brad Davis, "Vibrations of Steel-Framed Structural Systems Due to Human Activity Second Edition Steel Design Guide," 2016.

[13] S. Gagnon and C. Pirvu, Eds., *CLT Handbook: Cross-Laminated Timber*, U.S. Edition. Quebec, QC: FPInnovations, 2013.

[14] D. J. Ewins, *Modal Testing: Theory, Practice, and Application*, 2nd ed. Research Studies Press, 2000.

[15] D. J. Inman, *Engineering Vibration*, 4th ed. Pearson, 2014.

[16] P. Avitabile, "I Still Don't Understand Curvefitting... How Do You Get Mode Shapes From FRFs?," *SEM Experimental Techniques*, Apr. 1999.

[17] N. M. M. Maia and J. M. M. Silva, *Theoretical and Experimental Modal Analysis*. Research Studies Press, 1997.

[18] N. Labonnote, "Damping in Timber Structures," 2012. [Online]. Available: https://api.semanticscholar.org/CorpusID:108170378

[19] L. J. Hu, Y. H. Chui, and D. M. Onysko, "Vibration serviceability of timber floors in residential construction," *Progress in Structural Engineering and Materials*, vol. 3, no. 3, pp. 228–237, Jul. 2001, doi: 10.1002/pse.69.

[20] E. Ussher, K. Arjomandi, J. Weckendorf, and I. Smith, "Predicting effects of design variables on modal responses of CLT floors," *Structures*, vol. 11, pp. 40–48, Aug. 2017, doi: 10.1016/j.istruc.2017.04.006.

https://doi.org/10.52202/080513-0054